Biomagnetic monitoring and element content of lichen transplants in a mixed land use area of NE Italy

Danijela Kodnik [a], Aldo Winkler [b,*], Fabio Candotto Carniel [c], Mauro Tretiach [a]

[a] Università degli Studi di Trieste, Dipartimento di Scienze della Vita, Via L. Giorgieri 10, I-34127 Trieste, Italy
[b] Istituto Nazionale di Geofisica e Vulcanologia, Via di Vigna Murata 605, I-00143 Roma, Italy
[c] Università degli Studi di Trieste, Dipartimento di Scienze Chimiche e Farmaceutiche, Via L. Giorgieri 1, I-34127 Trieste, Italy

HIGHLIGHTS

- Lichen transplants allow easy and detailed environmental pollution data collection.
- Two-month exposed samples were enriched with magnetite-like magnetic minerals.
- Magnetic parameters and content of selected elements were correlated.
- Magnetic properties are good proxies also for low levels of heavy metal pollution.

GRAPHICAL ABSTRACT

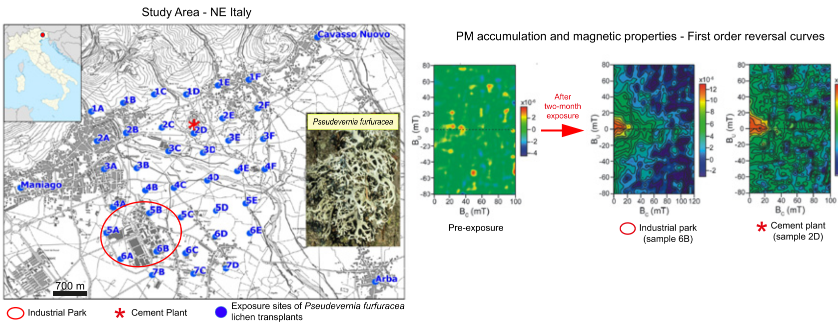

ARTICLE INFO

Accepted 28 March 2017

Editor: Elena Paoletti

Keywords:
Air pollution
Dust
Environmental magnetism
Magnetic properties
Particulate matter

ABSTRACT

The aim of this study was to verify whether it is possible to discriminate between the different pollution sources present in a mixed land use area of NE Italy on the basis of the magnetic properties and the element content of lichen transplants. Thalli of *Pseudevernia furfuracea* were collected in a pristine area of the South-Eastern Alps and exposed for 2 months in 40 sites located at the knots of a 700 m step grid covering ca. 40 km^2 of a mosaic of agricultural, forested, industrial and urban areas. In this way, the samples could be analyzed after a defined period of time, and compared to pre-exposure conditions. The post-exposure element content and the magnetic data substantially agreed, revealing a rather modest anthropogenic impact on the territory, mostly limited to an industrial park. Since the magnetic mineralogy was homogeneous throughout the entire set of samples, with magnetite-like minerals as the main magnetic carriers, it was not possible to discriminate between PM originating from the different pollution sources. The contribution given by the industrial park could be confirmed by the multivariate analysis of the element data set. Conversely, it was possible to assess the low environmental impact of the largest local industry, a cement plant, located outside the industrial park. Notwithstanding the relatively short time of the survey, *P. furfuracea* was proven to be an effective accumulator for biomagnetic monitoring studies, its magnetic properties being excellent proxies for heavy metal pollution even when the anthropogenic impact on the territory is low.

1. Introduction

Outdoor air-pollution is a major environmental and health problem. According to WHO (2014, 2016) fine particulate matter (PM) has the

* Corresponding author.
E-mail addresses: dkodnik@units.it (D. Kodnik), aldo.winkler@ingv.it (A. Winkler), fcandotto@units.it (F. Candotto Carniel), tretiach@units.it (M. Tretiach).

greatest effect on human health. It consists of a complex mixture of solid and liquid particles of organic and inorganic substances suspended in the air. It is associated with a broad spectrum of acute and chronic illnesses, such as lung cancer, chronic obstructive pulmonary disease and cardiovascular diseases. Particles with a diameter of 10 μm or less are the most health-damaging since they can penetrate deep inside the lungs.

Instrumental monitoring of PM requires expensive equipment, power availability and continuous maintenance, so it is impossible to apply a high-density sampling design when the environmental dispersion of airborne PM is influenced by numerous variables: sources, wind direction, topography, meteorological conditions. Biomonitoring with cryptogams (in particular, lichens and mosses) is an excellent technique that has frequently been used in the past decades to detect emission sources and distribution patterns of various airborne persistent pollutants (e.g. heavy metals, PAHs, dioxins, furans; Augusto et al., 2013, 2015; Bargagli and Mikhailova, 2002; Lucadamo et al., 2015; Nascimbene et al., 2014; Tretiach et al., 2007, 2011). Unlike plants, lichens and mosses lack a root system, and gas exchanges, absorption of nutrients and pollutants occur throughout the whole surface of the organism (Bargagli, 1998; Bargagli and Mikhailova, 2002; Garty, 2000). However, the use of cryptogams as biomonitors of PM pollution not always allows to verify with certainty the source of PM emission when several anthropogenic activities coexist in a relatively small area or when there is a mixed land use (Capozzi et al., 2016). For this purpose it may be useful to apply nitrogen, carbon, sulphur and heavy metal isotope fingerprints, since the analysis by mass spectrometer is an effective and sensitive method which needs very small quantities of material (e.g. Batts et al., 2004; Cloquet et al., 2009; Purvis et al., 2004; Spiro et al., 2004; Wadleigh, 2003; Wiseman and Wadleigh, 2002), but the analyses may be expensive and thus not always applicable on large sets of samples.

A further, promising method is the analysis of the magnetic properties of the airborne particulate matter. Previous studies demonstrated that aerosols have remarkable magnetic properties related to the content of magnetite-like ferrimagnetic particles (Flanders, 1994; Hunt et al., 1984), often associated to heavy metals such as Cd, Cr, Zn (Georgeaud et al., 1997; Hunt et al., 1984) and even to mutagenic organic compounds (Morris et al., 1995). Measurements of the magnetic properties of PM accumulated by tree leaves, tree bark and ring core samples, and by mosses and lichens have frequently been used as a proxy for PM pollution (e.g. Chaparro et al., 2013; Fabian et al., 2011; Gautam et al., 2005; Lehndorff et al., 2006; Moreno et al., 2003; Salo et al., 2012; Szönyi et al., 2007, 2008; Vuković et al., 2015; Zhang et al., 2006, 2008). Moreover, magnetic analyses are sensitive and allow the discrimination between different sources of pollution, according to the magnetic grain size, as pointed out in urban and traffic related contexts (Revuelta et al., 2014; Sagnotti et al., 2009). Unfortunately, it is also well known that the use of autochthonous organisms does not allow to refer the contamination to a defined period of time and, in particular, autochthonous lichens can incorporate atmospheric pollutants into their diamagnetic matrix over years (Marié et al., 2016). This drawback can be overcome by using transplants, since element composition and magnetic properties of the pre-exposure material can be carefully characterized. Furthermore, the use of transplants permits the coverage of those areas where autochthonous biomonitors are absent or rare (e.g. urban centers), and the low costs of the materials allow the application of a high-density sampling design (Kodnik et al., 2015). Finally, they are extremely useful to determine temporal patterns of airborne pollutants (Branquinho et al., 2008; Frati et al., 2005), because the exposure can be repeated as many times as it is requested, since it is not limited by the availability of autochthonous material. The magnetic properties of the PM accumulated by moss bags and lichen transplants were analyzed only sporadically (Salo et al., 2012; Salo, 2014; Salo and Mäkinen, 2014); Salo (2014) preliminary tested the effectiveness of the method by comparing the magnetic properties of PM accumulated by lichen and moss transplants and filter fabric, without cross-validating the results with the analysis of trace elements. More recently, Paoli et al. (2016) applied the method to autochthonous and transplanted lichens, considering also their elemental composition, with the samples exposed in single sites near a cement mill, a limestone quarry, a basalt quarry, an urban settlement, and an agricultural area. They were thus able to confirm that the geological characteristics of the substrate may strongly affect the magnetic properties of lichen thalli. On the basis of the results of the latter study, it can be argued that an integrated approach, in which the element content and the magnetic properties of lichens transplants are considered together, might be extremely useful to discriminate between emission sources, if a rigorous exposure design is applied. The topic is particularly relevant from the environmental point of view, because large areas of European countries are actually a mosaic of natural, agricultural, urban areas punctuated by industrial settlements, and the discrimination among different PM pollution sources often remains problematic.

Therefore, we decided to carry out the present study, with the main aim of testing the effectiveness of such an integrated approach. A mixed land use area was selected, for which we have a consistent series of environmental data derived from previous monitoring campaigns, respectively with: (*i*) autochthonous lichens (Tretiach and Baruffo, 2001; Tretiach and Pittao, 2008), concerning 10 trace elements; (*ii*) passive samplers, concerning PM and benzo(a)pirene (ARPA FVG, internal reports, in Ed.); (*iii*) lichen transplants (Kodnik et al., 2015), concerning 10 PAHs. In order to reduce subjectivity, the selected sampling method was systematic, with 40 exposure sites located at the knots of a 700 m step grid (Kodnik et al., 2015).

2. Material and methods

2.1. Study area

The study area is located in NE Italy (46°10′N 12°44′E; Fig. 1), at an elevation of 200–380 m a.s.l. It covers nearly 40 km^2, hosts a resident population of over 16,000 inhabitants (2015), and consists of the typical mixed land use patchwork that extends over large areas of N Italy, with natural, agricultural, urban, and industrial parks of different extension intermingled all together. The main potential pollution sources of the study area are: (*i*) an isolated, middle-sized cement plant (clinker production: 556,000 ton $year^{-1}$ in 2012; M. Vicenzetto, personal communication); (*ii*) a large industrial park; (*iii*) vehicular traffic, concentrated in the main urban centers and along a national road ("464 - Spilimbergo") that crosses the north part of the study area; (*iv*) agricultural activities, mostly related by ploughing (in late summer and in winter) and threshing (in summer); (*v*) domestic heating (in winter).

The selected sampling method was systematic, with 37 exposure sites located at the knots of a 700 m step grid, and 3 further sites located in the nearby urban centers of Arba, Cavasso Nuovo and Maniago (Fig. 1). The localization of the exposure sites in the study area was graphically represented using Quantum GIS 1.8.0. - Lisboa (2012).

The data on the meteorological conditions during the exposure period were retrieved from the closest weather station, located near Arba (Fig. 1). The total rainfall was 213.8 mm, given mostly by brief, intense summer storms. The mean air temperature was 24.6 °C, ranging from 19.3 to 30.2 °C (mean daily minimum and maximum, respectively). The winds were mainly north-northwesterly.

2.2. Lichen sampling, exposure and recovery

The epiphytic lichen *Pseudevernia furfuracea* (L.) Zopf. var. *furfuracea* was selected as a frequently used biomonitor of trace elements and PAHs (Gallo et al., 2014; Kodnik et al., 2015; Nascimbene et al., 2014; Tretiach et al., 2007, 2011). This lichen is relatively common, easy to identify, stress-tolerant, with a good resistance to transplantation

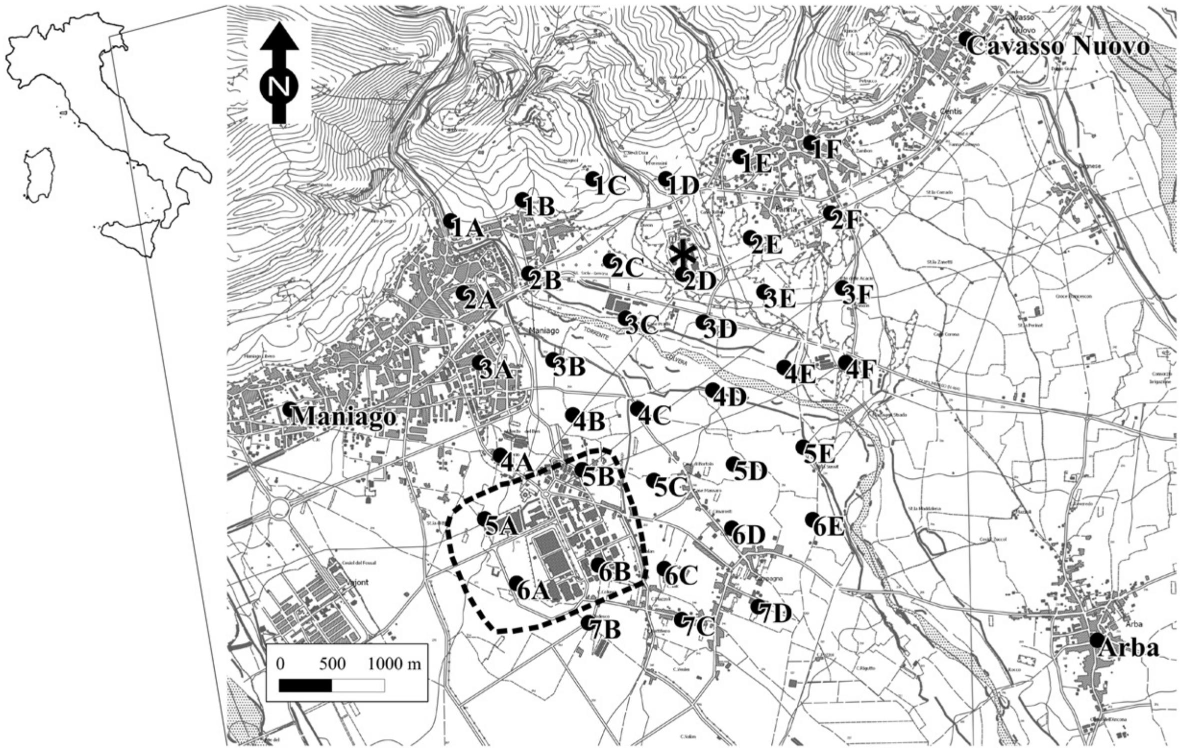

Fig. 1. Study area and localization of the 40 exposure sites. The cement plant is indicated by an asterisk, the industrial park by a closed dashed line.

(Tretiach et al., 2007), and morphologically prone to intercept particulate matter due to the development of a myriad of finger-like vegetative propagules ("isidia") (Tretiach et al., 2005). The pre-transplant samples were collected in the Carnic Alps (46°25′N 12°44′E) at ca. 1700 m a.s.l., far from any local pollution sources (Adamo et al., 2008; Tretiach et al., 2011), from branches of solitary larch (*Larix decidua* Mill.) trees at 2 to 4 m above the ground. The material was collected along with ca. 20 cm long piece of the supporting twig, transported to the laboratory in paper bags and left to dry out at room temperature. Moderately isidiate samples were selected avoiding those over-isidiate or with apothecia (because these structures may alter the surface/weight ratio of the thallus), infected by lichenicolous fungi or covered by epiphytic algae (Kodnik et al., 2015; Tretiach et al., 2007, 2011). Eight samples, each of them derived from at least six different thalli, were then randomly selected for the measurements of the pre-exposure values while the rest were prepared for exposure.

Each twig carrying 1–3 thalli was attached to a 120 cm long bamboo stick using plastic bonds (both first rinsed with distilled water) and sealed in plastic bags until exposure to avoid contamination.

The exposure was done on June 19th 2012, within 12 h of field work. In each site, two bamboo sticks were attached to the external branches of deciduous trees at approximately 4 m above the ground using plastic bonds. After two months, the samples were retrieved with a piece of the bamboo stick, sealed in individual plastic bags, and transported in a coolbag within 6 h to the laboratory, where the bags were opened, and the samples were left to dry out at room temperature (Kodnik et al., 2015). Samples of the sites 1E, 2C and 5B were lost during the exposure. Samples 4B and from Cavasso Nuovo had insufficient material for the measurement of the magnetic properties and were thus excluded from the statistical analyses as well.

2.3. Chemical analyses of the element content

A part of the most external lobe portions of each thallus was cut with porcelain scissors (ca. 1 g), pulverized in an agate mortar with liquid nitrogen, dried out over silica for 24 h and then sealed in Eppendorf containers until analysis (Tretiach et al., 2011). The samples were then digested with concentrated HNO_3, first cold then hot. After cooling, 6 ml of aqua regia were added per 1 g of sample and kept at 95 °C for 2 h, then the suspension was brought to volume (20 ml g^{-1}) by adding a 5% solution of HCl and filtered. The solution was then analyzed with a Perkin Elmer Elan 6000 ICP mass spectrometer for the following elements: Al, As, Bi, Ca, Cd, Co, Cr, Cu, Fe, Hg, K, Mn, Ni, Pb, Sb, Sn, V, Zn by ACME Analytical Laboratories (Vancouver, Canada), purposely selected as high-quality data provider for element content in different matrices, lichens included. The values were expressed on a dry mass basis (μg g^{-1}). Details on the ACME QA/QC protocol, which includes sample-prep blank carried through all stages of preparation and analysis, a pulp duplicate to monitor analytical precision, two reagent blanks to measure background and aliquots of in-house Standard Reference Materials like V16 and CDV-1 (plant leaves) to monitor accuracy, are given by Incerti et al. (2017). For comparative purposes, the accuracy of the analysis was verified by sending the "Certified Reference Material BCR-482 (*Pseudevernia furfuracea* (L.) Zopf), which was blindly analyzed in six samples. The recovery of the certified values of this material was as follows: Al 43%, As 84%, Cd 92%, Cr 99%, Cu 94%, Hg 87%, Ni 91%, Pb 92%, Zn 95%. The certified values for the standard were obtained using a different digestion protocol: a mixture of HNO_3 and HF at 100 °C for 14 h and 150 °C for 2 h (Quevauviller et al., 1996), which is why the recovery of Al was low.

2.4. Magnetic measurements

The remaining parts of the most external lobe portions of each lichen were cut with porcelain scissors and placed in pharmaceutical gel caps #4 (~0.15 ml) to determine their hysteresis properties and in standard 8 cm^3 plastic cubes for the magnetic susceptibility measurements. Gel cap samples were inserted into the carbon fiber probe for vibrating in the Princeton Measurement Corporation Micromag 3900 Vibrating Sample Magnetometer (VSM). Lichen fragments were carefully pressed inside the caps to reduce the interstices and to maximize the mass content. The coercive force (B_C), the saturation remanent magnetization

(M_{RS}) and the saturation magnetization (M_S) were determined using the VSM under cycling in a maximum field of 1.0 T and after subtracting the high field paramagnetic linear trend. The mass specific magnetization values for the concentration dependent parameters were calculated dividing the magnetic moments by the dry mass of the samples. The coercivity of remanence (B_{CR}) was determined from backfield remagnetization curves up to −1 T (after being magnetized in a positive 1 T field) and calculated as the average of the values extrapolated from logarithmic and linear backfield applications.

The magnetic grain size and the domain state of the PM accumulated by the lichens was investigated according to the theoretical hysteresis ratios (M_{RS}/M_S vs. B_{CR}/B_C) expected for magnetite in the "Day plot" (Day et al., 1977; Dunlop, 2002a, 2002b).

First order reversal curves (FORCs; see Pike et al., 1999; Roberts et al., 2000) were measured using the Micromag operating software, and processed, smoothed and drawn with the FORCINEL Igor Pro routine (Harrison and Feinberg, 2008). FORCs were measured in steps of 2.0 or 2.5 mT, with the averaging time ranging from 100 to 300 ms and the maximum applied field being 1.0 T. The optimum smoothing factor was evaluated by FORCINEL software.

The percentage decay of M_{RS} after 100 s was calculated as:

$$M_{RS}(SP)\% = 100 \times (M_{RS0} - M_{RS100})/M_{RS0};$$

where SP refers to the superparamagnetic fraction, M_{RS0} is the remanent magnetization measured as soon as the magnetic field is reduced to noise levels after the application of a 1 T field; M_{RS100} is the remanence measured 100 s later. The values of M_{RS} (SP) % are indicative of the contribution of the rapidly decaying viscous components of magnetization with respect to the overall remanent magnetization of the samples. These viscous components are usually carried by ultrafine magnetic particles, dimensionally in the superparamagnetic/stable single domain boundary, which is around 20–35 nm for magnetite (Butler and Banerjee, 1975; Sagnotti and Winkler, 2012; Wang et al., 2010).

The temperature dependency of the magnetic susceptibility, performed in air in the range 40 to 650 or 700 °C and back, was measured in an AGICO MFK-1 Kappabridge equipped with a CS-3 furnace and corrected for the susceptibility of the empty furnace; the mass magnetic susceptibility values are indicated with χ, and were calculated by the SAFYR measurement software.

The magnetic properties of a cement sample produced by the plant located at the center of the study area (Fig. 1) and of a dust sample directly collected from the filters located above the main furnace were also analyzed to test the magnetic similarity between the final products and the dusts bioaccumulated by the lichen transplants.

All the magnetic measurements were carried out at the palaeomagnetism laboratory of Istituto Nazionale di Geofisica e Vulcanologia, Rome (Italy).

2.5. Statistics

Descriptive statistics were performed using Microsoft Excel (Microsoft Office Professional Plus 2010). Principal component analysis (PCA), cluster analysis (tree clustering with Complete Linkage as the clustering method and 1-Pearson r as the linkage measure), Mann-Whitney *U* Test and Spearman's Rank correlation (p-value significant <0.05) were performed to verify differences between groups using STATISTICA 8.0 StatSoft Inc. (2007).

3. Results

3.1. Element content of the lichen transplants

Pre-exposure element concentrations in *P. furfuracea* thalli were within the ranges of background values of epiphytic lichens (Bargagli, 1998), being very similar to those of previous samples collected in the same pristine area (Adamo et al., 2008). The exposure modified significantly the content of most elements (Al, As, Bi, Ca, Cd, Cu, Fe, K, Ni, Pb, Sb, Sn; Mann-Whitney *U* Test, for p-value <0.05; Table 1).

The tree diagram of the elements (Fig. 2) consists of 5 main groups. Mn, V and K (group 1 of Fig. 2) were partially leached from the exposed thalli, i.e. their post-exposure content was lower than the pre-exposure value. Cr, Ni, Co, and Sn (group 2) showed a slight increment (statistically significant for Ni and Sn), often with a maximum in site 6A (industrial zone; Fig. 1). As and Al (groups 3 and 4, respectively) had peculiar distribution patterns in the study area, which differ from those of all the other elements. Group 5 gathers elements with heterogeneous

Table 1
Element content (μg g^{-1}), mass magnetic susceptibility (χ; 10^{-8} m^3 kg^{-1}), mass saturation remanent magnetization (M_{RS}; mAm^2 kg^{-1}), mass saturation magnetization (M_S; mAm^2 kg^{-1}), coercivity of remanence (B_{CR}; T) and coercive force (B_C; T) measured in pre- and post-exposure samples of the lichen *Pseudevernia furfuracea* transplanted for two months in the sites of Fig. 1. (n = number of samples; S.D. = standard deviation; C.V. = coefficient of variation).

	pre-exposure (n = 8)					**post-exposure** (n = 35)				
	mean	S.D.	C.V.	min	max	mean	S.D.	C.V.	min	max
Al	130.00	48.30	37%	100.00	200.00	213.51	34.66	16%	200.00	300.00
As	0.10	0.00	0%	0.10	0.10	0.22	0.14	64%	0.10	0.50
Bi	0.09	0.06	67%	0.04	0.21	0.05	0.04	88%	0.02	0.27
Ca	3,330.00	326.77	10%	2,900.00	3,800.00	4,494.59	1,754.67	39%	2,300.00	11,400.00
Cd	0.12	0.01	10%	0.10	0.14	0.15	0.03	23%	0.10	0.27
Co	0.14	0.04	26%	0.09	0.21	0.16	0.04	22%	0.08	0.24
Cr	2.33	0.51	22%	1.90	3.30	2.44	0.55	23%	1.00	4.30
Cu	4.45	0.63	14%	3.93	5.51	6.02	1.10	18%	4.48	8.29
Fe	169.00	43.58	26%	130.00	250.00	253.24	63.29	25%	170.00	440.00
Hg	0.13	0.02	18%	0.10	0.17	0.13	0.03	21%	0.09	0.20
K	2,830.00	605.62	21%	2,400.00	3,800.00	2,272.97	359.51	16%	1,800.00	3,300.00
Mn	96.90	7.05	7%	90.00	112.00	88.16	27.08	31%	47.0	161.00
Ni	0.83	0.26	32%	0.50	1.3	1.07	0.34	32%	0.70	2.30
Pb	3.00	0.41	14%	2.27	3.41	3.51	0.63	18%	2.46	5.14
Sb	0.08	0.01	9%	0.07	0.09	0.11	0.02	20%	0.07	0.19
Sn	0.28	0.03	12%	0.24	0.33	0.35	0.07	21%	0.23	0.55
V	4.10	1.73	42%	2.00	6.00	3.84	1.17	30%	2.00	7.00
Zn	33.38	1.45	4%	31.20	36.6	35.00	4.94	14%	25.60	42.60
χ	0.467	0.444	95%	0.118	1.490	1.798	1.355	75%	0.350	7.409
M_{RS}	0.151	0.055	36%	0.071	0.243	0.269	0.131	49%	0.068	0.797
M_S	0.754	0.102	14%	0.660	0.972	2.234	1.168	52%	0.948	6.548
B_{CR}	0.041	0.008	20%	0.031	0.055	0.039	0.004	11%	0.031	0.048
B_C	0.017	0.004	23%	0.012	0.025	0.012	0.003	25%	0.006	0.020

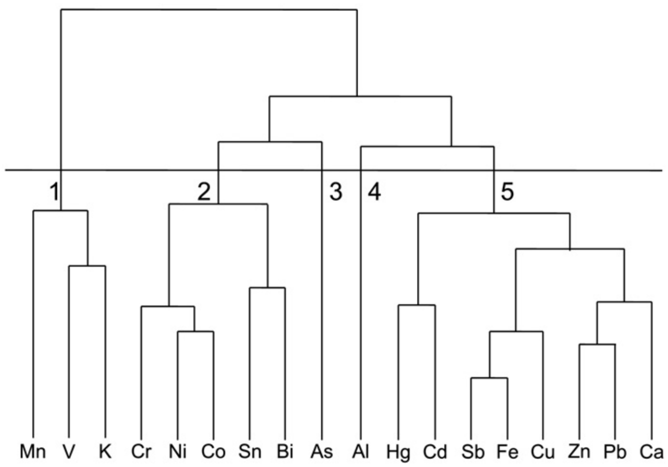

Fig. 2. Tree diagram of the elements measured in the samples of the lichen *Pseudevernia furfuracea* after the two-month exposure in the 40 sites of Fig. 1. The data are normalized on the mean of pre-exposure values as follows: [(post-exposure − pre-exposure) / pre-exposure].

distribution on the territory, but with a significant increase in post-exposure concentration, particularly high for Cd, Sb, Fe, Cu, Pb and Ca, with maxima frequently located in 6B (industrial park, e.g. Sb, Fe, Cu).

3.2. Magnetic properties of the lichen transplants

The mass specific values of χ, M_S and M_{RS} (Table 1) have been normalized on the mean pre-exposure values as: [(post-exposure − pre-exposure) / pre-exposure], and they are shown in Fig. 3a; B_C and B_{CR} values are shown in Table 1 and Fig. 3b.

The pre-exposure samples had very weak but measurable concentration dependent magnetic properties, always lower than the post-exposure samples; the highest post-exposure values were found in the samples 6A and 6B, from the industrial park.

B_C and B_{CR} are homogeneous over the whole set; B_{CR} is <0.050 T for most of the samples, indicating the prevalence of low-coercivity magnetic minerals.

The shapes of the hysteresis loops (Fig. 4a, c), of the isothermal remanent magnetization (IRM) acquisition and of the back-field curves (Fig. 4b, d) of the samples 2D (cement plant) and 6A (industrial park) are similar, suggesting a common ferromagnetic *sl* mineralogy. Higher values of the concentration dependent parameters are probably given by higher concentrations of analogous ferromagnetic *sl* particles accumulated by the lichens exposed in the industrial park. It is difficult to estimate the M_{RS} decay in 100 s because of the large measurement errors due to the low remanent magnetization values. However, a clear decay is not evident after 100 s (Fig. S1a, b), indicating that in both samples the rapidly decaying components of magnetization should be negligible. The variation of the magnetic susceptibility vs. temperature is shown in Fig. S2a, b for the samples 6B (industrial park) and 2D (cement plant), respectively; black circles represents the heating, white circles the following cooling to room temperature. The curves are noisy and somewhat difficult to read, because of the weak susceptibility and the prevailing lichen matrix on the overall volume of the sample. For both samples, the Hopkinson peak precedes the decrease of susceptibility up to around 580 °C, indicating that the main magnetic mineral is magnetite.

The "Day plot" (Fig. 5) shows that the most of the samples fall in the central pseudo single domain (PSD) region of the plot, which can depend on a broad mixture of single domain (SD), or even superparamagnetic (SP) particles, up to multi-domain (MD) magnetite grains. In general, the data fall between the theoretical curves calculated for mixtures of single domain and multidomain magnetite grains and

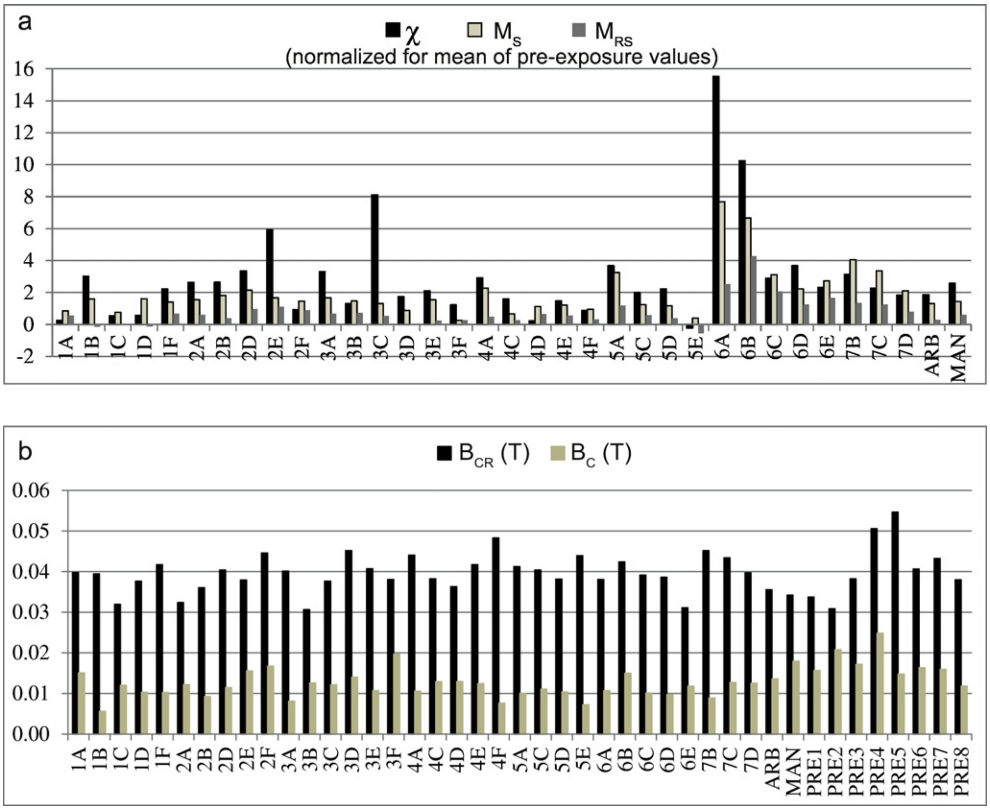

Fig. 3. Histograms of mass specific χ, M_S, M_{RS} (a) measured in pre- and post-exposure samples of the lichen *Pseudevernia furfuracea* transplanted for two months in the sites of Fig. 1 and normalized on the mean of pre-exposure values as follows: [(post-exposure − pre-exposure) / pre-exposure]. Histograms of B_{CR} (T) and B_C (T) are in (b).

those evaluated for mixtures of SD and SP magnetite particles (Dunlop, 2002a,b).

The samples 6A and 6B (industrial park) are within the cluster of points in the central region of the plot, together with the sample 2D (cement plant) and most of the pre-exposure samples.

The critical magnetic grain size transitions, theoretically determined for equidimensional magnetite, are about 0.03 μm for SP to SD, 0.08 μm for SD to PSD, 17 μm for PSD to true MD (Butler and Banerjee, 1975).

FORC diagrams of samples 2D, 6B and of a pre-exposure sample are shown in Fig. 6; although they are very noisy, PSD (even if the discrimination between a SD-MD mixture and PSD is not straightforward; Roberts et al., 2000) and fine MD low-coercivity features emerge for both samples, whereas no relevant magnetic components are present in the pre-exposure sample. FORC diagrams thus confirm the features pointed out by the "Day Plot" diagram and highlight the accumulation of magnetic particles in the post-exposure samples.

3.3. Magnetic analyses of the cement and dust sample

The hysteresis loop, the IRM acquisition and the back-field application curves of the cement sample are shown in Fig. 4e and f, respectively. The decay of M_{RS} in 100 s (Fig. S1c) suggests the presence of viscous components of magnetization, contributing about 10% to the overall remanent magnetization.

The thermomagnetic curve (Fig. S2c) is much better defined, with respect to those of the samples 6B and 2D (Fig. S2a, b), due to the higher values of the magnetic susceptibility. The main decrease of the magnetic susceptibility occurs from about 400 °C to 580 °C, which can be ascribed, respectively, to the relevant presence of maghemite (which inverts to hematite upon heating) and to magnetite, and continues up to 680 °C, the Néel temperature for hematite; the Hopkinson peak is absent. Overall, the presence of a heterogeneous mix of iron oxides is suggested. The magnetic grain size of the cement sample, when referred to magnetite (Fig. 5), does not seem to differ from the lichen sample data and falls into the central region of the "Day plot" as well.

Noticeably higher mass specific M_S and M_{RS} values, with respect to the lichens, have been determined (0.11 Am^2 kg^{-1} and 0.02 Am^2 kg^{-1}, respectively) also in the dust samples collected from the filters located above the main furnace. The main drop of magnetic susceptibility in the thermomagnetic curve (Fig. S2d) occurs up to about 580 °C and continues, changing slope, until about 620 °C, indicating the presence of maghemite and/or hematite, in addition to magnetite, as suggested by the thermomagnetic analysis of different kinds of industrial fly ashes, including cement plants (Magiera et al., 2011; Magiera et al., 2013; Paoli et al., 2016). In this case, the Hopkinson peak is well-defined, and the cooling curve indicates the formation of new magnetite during the heating process.

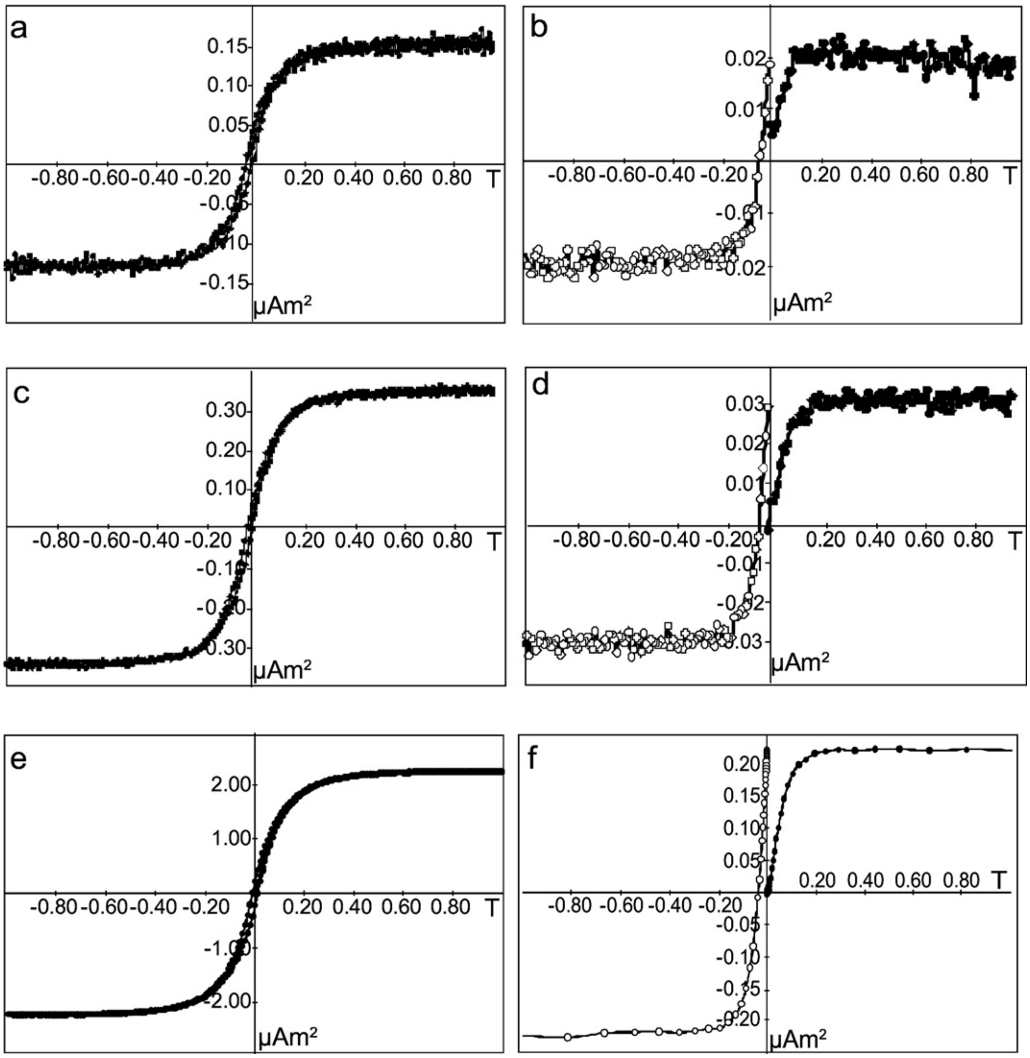

Fig. 4. Hysteresis loops (a, c), isothermal remanent magnetization (IRM) acquisition and back-field application curves (b, d) of *Pseudevernia furfuracea* transplanted for two months in the sites 2D (a, b; cement plant) and 6A (c, d; industrial park) of Fig. 1; (e) hysteresis loop and (f) IRM acquisition/back-field application curves of the cement sample. Hysteresis loops are corrected for the high-field linear trend; black circles indicate IRM acquisition.

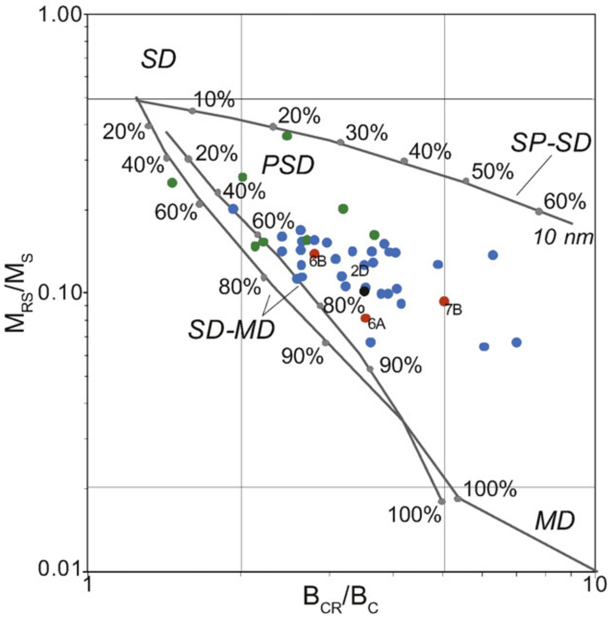

Fig. 5. Bi-logarithmic "Day plot" of the hysteresis ratios M_{RS}/M_S vs. B_{CR}/B_C for samples of the lichen *Pseudevernia furfuracea* transplanted for two months in the sites of Fig. 1, and of the pre-exposure samples (red symbols – industrial park; green – pre-exposure; black – cement; light-blue – all the other samples). The SD (single domain), PSD (pseudo-single domain) and MD (multidomain) fields and the theoretical mixing trends for SD-MD and SP-SD grains (SP, superparamagnetic) are from Dunlop (2002a, 2002b) and refer to magnetite.

3.4. Data statistics

The principal component analysis (PCA) was based on the mass specific values of the variables χ, M_{RS}, M_S, and post-exposure element content, both normalized with respect to the mean pre-exposure values (see above). The PCA representative plot is shown in Fig. 7a, and the corresponding loading plot in Fig. 7b.

Pronounced differences are evident among the samples. The sample 1D, located at one end of the first component, segregates from all the other samples. It was exposed in a forested area and has low levels of contamination, as shown also by the corresponding loading plot in Fig. 7b. On the contrary, the samples 6A and 6B, from the industrial park, are located at the opposite end of the first component of Fig. 7a and, as previously seen, they had the highest levels of contamination for several elements (Cr, Cu, Fe, Ni, Sb) and the highest values of concentration dependent magnetic parameters (Fig. 7b).

Spearman's Rank correlation between χ, $M_{S,}$ M_{RS} (mass specific values) and element concentration was tested (Table 2). Significant positive correlations have been found between the concentrations of Cu, Fe, Ni, Sn and χ, M_S and M_{RS}. The elements Cd and Co correlated only to χ, while Bi, Ca, Sb and Zn to M_S and/or M_{RS}. These deviations in the significance of the correlations between elemental concentration data and concentration dependent magnetic parameters may also depend on large relative errors due to their generally low and sometimes barely measurable values. Significant negative correlations were found between K, Mn, V and χ, M_S and/or M_{RS}, which is due to their partial leakage from the samples.

4. Discussion

Most of the works dealing with the magnetic properties of PM intercepted by biomonitors have been carried out on leaves of seed plants, generally trees or shrubs, more rarely on autochthonous cryptogams (mosses and/or lichens) (e.g. Chaparro et al., 2013; Fabian et al., 2011; Jordanova et al., 2010; Szönyi et al., 2007, 2008). In the intercomparison carried out by Jordanova et al. (2010), lichens and mosses were found to have the strongest contrast between clean and polluted environment, a further proof – if needed – that these cryptogams are very good biomonitors of PM. The lack of sufficient biological material in the most polluted sites, characterized by a true "lichen and moss desert", can require the application of the transplant technique: suitable species are collected from pristine sites and are exposed in the target areas for assessing air pollutant depositions.

With the transplant technique, a critical point is the characteristics of the pre-exposure material. Typically, the material is collected in pristine areas, far from known pollution sources, and therefore it should have a baseline content for most of the elements. In prevision of a enviromagnetic survey, the material should have very low magnetic susceptibility values; magnetic susceptibility is directly measurable even in the field and can be interpreted as a bulk indicator of the concentration of magnetic minerals. The mass susceptibility values reported in the literature range between 3.4 and 3.9×10^{-8} m^3 kg^{-1} for *Hypogymnia physodes* (L.) Nyl. (Salo, 2014; Salo et al., 2012), 1.33 $\times 10^{-8}$ m^3 kg^{-1} for *Evernia prunastri* (L.) Ach. (one sample; Paoli et al., 2016) between 14.3 and 41.0×10^{-8} m^3 kg^{-1} for other foliose and microfoliose lichens (Chaparro et al., 2013) and between −1.0–1.0×10^{-8} m^3 kg^{-1} for mosses (Salo, 2014; Salo et al., 2012; Salo and Mäkinen, 2014). In Jordanova et al. (2010) lichens and mosses were considered together, and much higher and more variable χ background

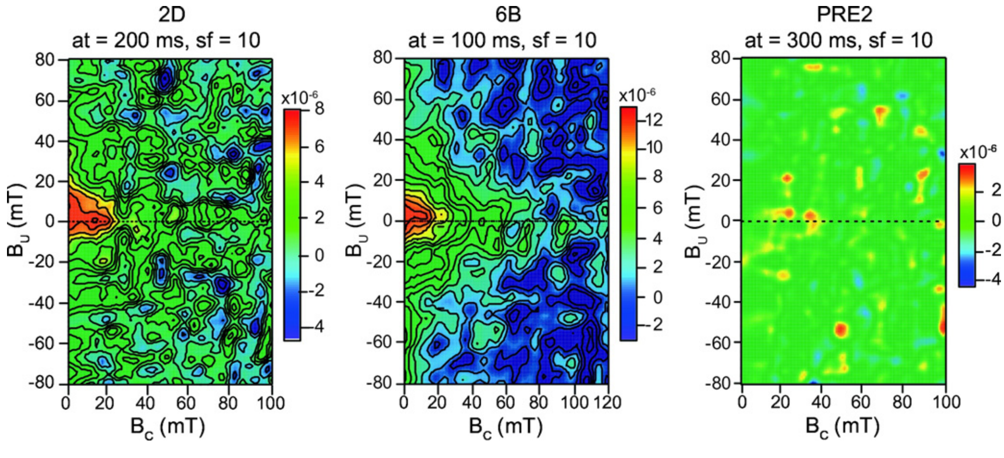

Fig. 6. FORC (First Order Reversal Curve) diagrams for samples 2D and 6B of the lichen *Pseudevernia furfuracea* transplanted for two months in the sites of Fig. 1, and of a pre-exposure sample (PRE2); "at" indicates the selected averaging time and "sf" the calculated optimum smoothing factor.

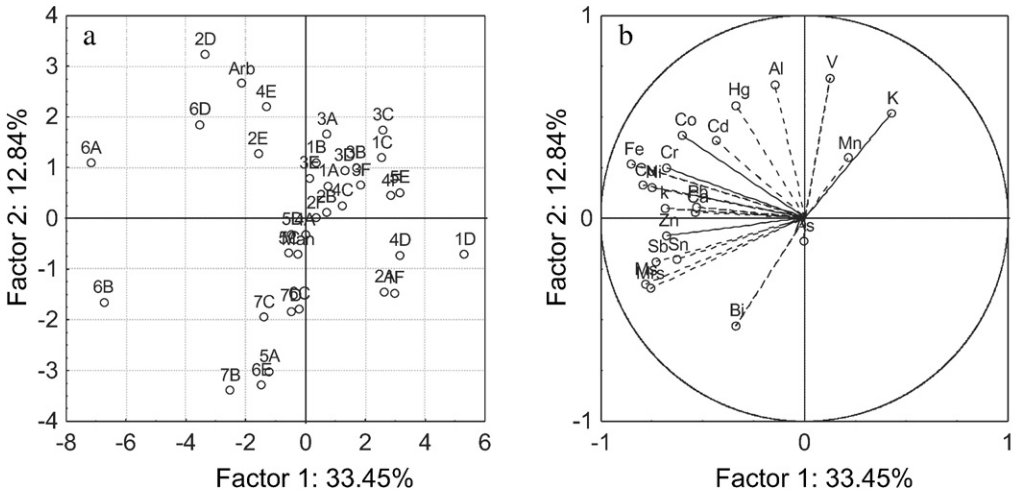

Fig. 7. Principal component analysis of the samples of *Pseudevernia furfuracea* after the two-month exposure in the 40 sites of Fig. 1, based on the values of mass specific χ, M_S, M_{RS} and the element content, both normalized on the mean pre-exposure values as [(post-exposure − pre-exposure) / pre-exposure] (a), and the corresponding loading plot (b).

levels were observed ($9.18–86.8 \times 10^{-8}$ m^3 kg^{-1}), but it should be kept in mind that in the latter study sampling was extended to epilithic and epigaeic species, and therefore the wider range of values is not a surprise, being related to a stronger contamination by soil particles. In comparison to these works, our pre-exposure samples had very low levels of χ ($0.118–1.490 \times 10^{-8}$ m^3 kg^{-1}; Table 1) and, according to the FORC diagram (Fig. 6), the magnetic fraction was not relevant. This confirms that the Alpine area we repeatedly visited for sampling (Adamo et al., 2008; Kodnik et al., 2015; Tretiach et al., 2007, 2011) has a very low anthropogenic or natural impact, in accordance to the very low element concentrations (Table 1), that are fully in line with the results of a recent sampling extended to whole Italy, aimed at pinpointing true “background” areas (Capozzi et al., 2015; Incerti et al., 2017).

If the pre-exposure values were low, both in term of element content and enviromagnetic properties, our post-exposure data sets suggest a modest anthropogenic impact on the environment. In comparison to other surveys carried out with the same technique throughout Italy (see e.g. Gallo et al., 2014; Giordano et al., 2005; Sorbo et al., 2008), but even in the same area, in a different period of the year (unpubl. results), the element concentration enrichment observed after the two-month exposure was certainly low, and this was also reflected by the post-exposure values of the mass magnetic susceptibility, which ranged between 0.350 and 7.409×10^{-8} m^3 kg^{-1} (Table 1). On the contrary, after a six-month exposure of *H. physodes* transplants around a cluster of heavy metal and chemical industries, including a Cu-Ni smelter complex, Salo (2014) observed χ values ranging between 0.7 and 77.2 $\times 10^{-8}$ m^3 kg^{-1}, whereas moss bags exposed in the same area reached higher values already after only two months (0.2–186.7 $\times 10^{-8}$ m^3 kg^{-1}) (Salo et al., 2012), and after a six-month exposure reached a maximum of 127.3×10^{-8} m^3 kg^{-1} (Salo, 2014) and 408.5 $\times 10^{-8}$ m^3 kg^{-1} (Salo and Mäkinen, 2014).

One reason for the modest increase observed in this study could be the meteorological conditions during the exposure period. Although the total rainfall was not particularly abundant, it occurred in form of several brief and intense thunderstorms that might have caused a wash effect of the PM accumulated on the surface of the lichens. This is partially confirmed by the leakage of Mn, K and V observed in the exposed transplants. However, the slight, but statistically significant increase of some elements and of magnetic susceptibility observed in most of the exposed lichen samples also indicates that there was actually an enrichment, mostly of anthropogenic origin. This conclusion is supported by the fact that the soil–related elements (e.g. aluminum) remained very low, and maxima were never observed in exposure sites belonging to the agricultural stratum, whereas the highest increase was concentrated in the sites within or immediately near the industrial park, confirming previous results (Tretiach and Baruffo, 2001; Tretiach and Pittao, 2008). According to the data made available by the local authorities, the activities potentially consistent with the observed high levels of Cr, Cu, Fe, Ni and Sb, are various: one electroplating factory which works brass, bronze, copper, nickel and zinc; two gray cast iron and steel smelters; several forging factories; several knife manufacturing factories.

Although the post-exposure enrichment in PM was generally low, the magnetic analysis revealed some interesting traits that complemented the information derived from the elemental analysis. The magnetic mineralogy was reasonably homogenous in the whole set of samples and, crossing hysteresis, FORC and “Day Plot” data, magnetite-like ferrimagnetic grains, mostly in PSD up to fine MD domain state and, by implication, grain size range, resulted to be the main magnetic carriers. Thus, it was not possible to distinguish between the cement plant and the industrial dusts on the basis of the magnetic grain size.

This type of magnetic PM can be associated to industrial, domestic or vehicle emissions (Flanders, 1994; Hunt et al., 1984), abrasion products

Table 2
Spearman's Rank correlation between χ, M_S, M_{RS} (mass specific values) and element concentration measured in the post-exposure samples of the lichen *Pseudevernia furfuracea* transplanted for two months in the sites of Fig. 1. The data are normalized on the mean of pre-exposure values as follows: [(post-exposure − pre-exposure) / pre-exposure] (correlations considered significant for p-value < 0.05 are marked in bold).

	χ	M_S	M_{RS}
Al	0.079243	-0.231308	-0.210043
As	-0.073530	-0.178698	-0.173718
Bi	0.247147	**0.386490**	**0.469923**
Ca	0.278346	**0.355711**	0.262088
Cd	**0.367551**	0.101379	0.189400
Co	**0.338681**	0.172294	0.074122
Cr	0.267275	0.271247	0.266849
Cu	**0.470020**	**0.347296**	**0.363827**
Fe	**0.447875**	**0.414997**	**0.341198**
Hg	0.187014	-0.066541	0.063599
K	-0.209411	**-0.364811**	**-0.516546**
Mn	**-0.348112**	-0.233663	**-0.394761**
Ni	**0.412132**	**0.469807**	**0.397891**
Pb	0.013307	0.016809	0.131671
Sb	0.329672	**0.471809**	**0.398690**
Sn	**0.564233**	**0.548096**	**0.528311**
V	-0.159548	**-0.341375**	-0.260595
Zn	0.315170	**0.336041**	**0.347248**

from asphalt and from vehicles brake systems (Hoffmann et al., 1999, Sagnotti et al., 2009) or industrial activities such as smelters (Salo and Mäkinen, 2014). Coarser and angular-shaped particles are often the result of abrasion in traffic related powders, while iron-rich spherules are predominant in industrial and urban combustion patterns (Sagnotti et al., 2009; Salo et al., 2012). In the study area vehicle traffic is not particularly intense since there are no large urban centers present, however domestic heating by wood burning during the winter period can be an important source of airborne particulate matter in the city centers that is not detectable during summer, when this study was conducted (Kodnik et al., 2015; WHO, 2005).

Clinker production, that is the core of the industrial processes of the cement plant present at the center of our study area, far from the industrial park, occurs at high temperatures (1400–1500 °C) when a mixture of magnetite and hematite is generated (Flanders, 1994; Hansard et al., 2011, 2012; Magiera et al., 2011; Petrovský and Ellwood, 1999). Hematite was not evident in the lichen transplants while, according to magnetic mineralogy data, it was present in the cement sample and, less obviously, in the dust sample collected from the filters located above the main furnace. Moreover, no particular metal enrichment, both from the chemical and magnetic point of views, was found in the samples exposed in and around the cement plant, so that it might be concluded that this has a very low environmental fingerprint.

Finally, from the methodological point of view, it can be underlined that the significant correlations observed between the concentration dependent magnetic parameters and the elements Cu, Fe, Ni, Sn, Cd, Co, Bi, Sb and Zn support the concentration dependent magnetic properties as excellent proxies for heavy metal pollution even at low contamination levels (Table 2).

5. Conclusions

In this multidisciplinary survey, the main pollution source resulted to be the industrial park located in the SW corner of the study area. The concentrations of selected elements and the concentration dependent magnetic properties were, in that sense, in substantial agreement. The magnetic mineralogy was homogeneous throughout the entire set of samples; the main magnetic carriers resulted magnetite-like minerals, mostly in pseudo-single domain up to fine multidomain grain size range. The cement plant was excluded as the main source of airborne particulate matter, and no strict connection was found by comparing the magnetic mineralogy of the cement and dust samples therein produced with respect to the post-exposure PM intercepted by the lichen samples. From this point of view, the transplants of *Pseudevernia furfuracea* have proven to be effective for carrying out biomagnetic measurements; the two-month exposure was sufficient for them to accumulate enough PM for a detailed magnetic characterization, proving that the magnetic properties are excellent proxies for heavy metal pollution even when the anthropogenic impact on the territory is rather modest.

Moreover, with a regular grid of lichen transplants it is possible to investigate the variations of their magnetic properties according to the exposure period and their initial conditions, with the additional possibility of covering unvegetated areas, thus bypassing the limits of magnetic measurements on native biological samples.

Acknowledgements

Field work and element analysis was financed by Cementizillo S.p.A. (Padova, Italy) to M. T. as scientific responsible. The activity of D. K. was funded by a Cementizillo S.p.A. (Padova, Italy) PhD grant. The sponsor influenced neither the study design, analysis and interpretation of data, nor the decision to submit the article for publication. A. W. would like to thank Donatella Abbruzzese, Teresa Lapera and Veronica Valle for the involvement during their stage at INGV.

The recommendations by the Associate Editor, Elena Paoletti and three anonymous reviewers helped to improve the manuscript.

References

Adamo, P., Bargagli, R., Giordano, S., Modenesi, P., Monaci, F., Pittao, E., Spagnuolo, V., Tretiach, M., 2008. Natural and pre-treatments induced variability in the chemical composition and morphology of lichens and mosses selected for active monitoring of airborne elements. Environ. Pollut. 152, 11–19.
Augusto, S., Máguas, C., Branquinho, C., 2013. Guidelines for biomonitoring persistent organic pollutants (POPs), using lichens and aquatic mosses – a review. Environ. Pollut. 180, 330–338.
Augusto, S., Pinho, P., Santosa, A., Botelhoc, M.J., Palma-Oliveirac, J., Branquinho, C., 2015. Declining trends of PCDD/Fs in lichens over a decade in a Mediterranean area with multiple pollution sources. Sci. Total Environ. 508, 95–100.
Bargagli, R., 1998. Lichens as biomonitors of airborne trace elements. In: Bargagli, R. (Ed.), Trace Elements in Terrestrial Plants: An Ecophysiological Approach to Biomonitoring and Biorecovery. Springer-Verlag, Berlin Heidelberg, New York, pp. 179–206.
Bargagli, R., Mikhailova, I., 2002. Accumulation of inorganic contaminants. In: Nimis, P.L., Scheidegger, C., Wolseley, P.A. (Eds.), Monitoring With Lichens – Monitoring Lichens. Nato Science Series, pp. 65–84.
Batts, J.E., Calder, L.J., Batts, B.D., 2004. Utilizing stable isotope abundances of lichens to monitor environmental change. Chem. Geol. 204, 345–368.
Branquinho, C., Gaio-Oliveira, G., Augusto, S., Pinho, P., Máguas, C., Correia, O., 2008. Biomonitoring spatial and temporal impact of atmospheric dust from a cement industry. Environ. Pollut. 151, 292–299.
Butler, R.F., Banerjee, S.K., 1975. Theoretical single-domain grain size range in magnetite and titanomagnetite. J. Geophys. Res. 80, 4049–4058.
Capozzi, F., Cecconi, E., Adamo, P., Bargagli, R., Benesperi, R., Bidussi, M., Candotto, Carniel F., Craighero, T., Cristofolini, F., Giordano, S., Panepinto, F., Puntillo, D., Ravera, S., Spagnuolo, V., Tretiach, M., 2015. Contenuto elementare nei talli del lichene epifita *Pseudevernia furfuracea* (L.) Zopf raccolti in aree remote d'Italia. Notiziario della Società Lichenologica Italiana. 28 p. 18.
Capozzi, F., Giordano, S., Di Palma, A., Spagnuolo, V., De Nicola, F., Adamo, P., 2016. Biomonitoring of atmospheric pollution by moss bags: discriminating urban-rural structure in a fragmented landscape. Chemosphere 149, 211–218.
Chaparro, M.A., Lavornia, J.M., Chaparro, M.A., Sinito, A.M., 2013. Biomonitors of urban air pollution: magnetic studies and SEM observations of corticolous foliose and microfoliose lichens and their suitability for magnetic monitoring. Environ. Pollut. 172, 61–69.
Cloquet, C., De Muynck, D., Signoret, J., Vanhaecke, F., 2009. Urban/peri-urban aerosol survey by determination of the concentration and isotopic composition of Pb collected by transplanted lichen *Hypogymnia physodes*. Environ. Sci. Technol. 43, 623–629.
Day, R., Fuller, M., Schmidt, V.A., 1977. Hysteresis properties of titanomagnetites: grain-size and compositional dependence. Phys. Earth Planet. Inter. 13, 260–267.
Dunlop, D.J., 2002a. Theory and application of the Day plot (M_{RS}/M_S versus H_{CR}/H_C) 1. Theoretical curves and tests using titanomagnetite data. J. Geophys. Res. 107. http://dx.doi.org/10.1029/2001JB000486.
Dunlop, D.J., 2002b. Theory and application of the day plot (M_{RS}/M_S versus H_{CR}/H_C) 2. Application to data for rocks, sediments, and soils. J. Geophys. Res. 107. http://dx.doi.org/10.1029/2001JB000487.
Fabian, K., Reimann, C., McEnroe, S.A., Willemoes-Wissing, B., 2011. Magnetic properties of terrestrial moss (*Hylocomium splendens*) along a north-south profile crossing the city of Oslo, Norway. Sci. Total Environ. 409, 2252–2260.
Flanders, P.J., 1994. Collection, measurement, and analysis of airborne magnetic particulates from pollution in the environment. J. Appl. Phys. 75, 5931–5936.
Frati, L., Brunialti, G., Loppi, S., 2005. Problems related to lichen transplants to monitor trace element deposition in repeated surveys: a case study from central Italy. J. Atmos. Chem. 52, 221–230.
Gallo, L., Corapi, A., Loppi, S., Lucadamo, L., 2014. Element concentrations in the lichen *Pseudevernia furfuracea* (L.) Zopf transplanted around a cement factory (S Italy). Ecol. Indic. 46, 566–574.
Garty, J., 2000. Environmental and element content in lichens. In: Markert, B., Friese, K. (Eds.), Trace Elements - Their Distribution and Effects in the Environment. Elsevier Science, Amsterdam, pp. 245–276.
Gautam, P., Blaha, U., Appel, E., 2005. Magnetic susceptibility of dust-loaded leaves as a proxy of traffic-related heavy metal pollution in Kathmandu city, Nepal. Atmos. Environ. 39, 2201–2211.
Georgeaud, V.M., Rochette, P., Ambrosi, J.P., Vandamme, D., Williamson, D., 1997. Relationship between heavy metals and magnetic properties in a large polluted catchment: the Etang de Berre (south of France). Phys. Chem. Earth 22, 211–214.
Giordano, S., Adamo, P., Sorbo, S., Vigniani, S., 2005. Atmospheric trace metal pollution in the Naples urban area based on results from moss and lichen bags. Environ. Pollut. 136, 431–442.
Hansard R, Maher, B.A., Kinnersley, R.P., 2011. Biomagnetic monitoring of industry-derived particulate pollution. Environ. Pollut. 159, 1673–1681.
Hansard R, Maher, B.A., Kinnersley, R.P., 2012. Rapid magnetic biomonitoring and differentiation of atmospheric particulate pollutants at the roadside and around two major industrial sites in the U.K. Environ. Sci. Technol. 46, 4403–4410.
Harrison, R.J., Feinberg, J.M., 2008. FORCinel: an improved algorithm for calculating first-order reversal curve distributions using locally weighted regression smoothing. Geochem. Geophys. Geosyst. 9. http://dx.doi.org/10.1029/2008GC001987.
Hoffmann, V., Knab, M., Appel, E., 1999. Magnetic susceptibility mapping of roadside pollution. J. Geochem. Explor. 66, 313–326.
Hunt, A., Jones, J., Oldfield, F., 1984. Magnetic measurements and heavy metals in atmospheric particles of anthropogenic origin. Sci. Total Environ. 33, 129–139.
Incerti, G., Cecconi, E., Capozzi, F., Adamo, P., Bargagli, R., Benesperi, R., Candotto, Carniel F., Cristofolini, F., Giordano, S., Puntillo, D., Spagnuolo, V., Tretiach, M., 2017. Infraspecific variability in baseline element composition of the epiphytic lichen *Pseudevernia*

furfuracea in remote areas: implications for biomonitoring of air pollution. Environ. Sci. Pollut. Res. http://dx.doi.org/10.1007/s11356-017-8486-7 (in press).
Jordanova, D., Petrov, P., Hoffmann, V., Gocht, T., Panaiotu, C., Tsacheva, T., Jordanova, N., 2010. Magnetic signature of different vegetation species in polluted environment. Stud. Geophys. Geod. 54, 417–442.
Kodnik, D., Candotto, Carniel F., Licen, S., Tolloi, A., Barbieri, P., Tretiach, M., 2015. Seasonal variations of PAHs content and distribution patterns in a mixed land use area: a case study in NE Italy with the transplanted lichen *Pseudevernia furfuracea*. Atmos. Environ. 113, 255–263.
Lehndorff, E., Urbat, M., Schwark, L., 2006. Accumulation histories of magnetic particles on pine needles as function of air quality. Atmos. Environ. 40, 7082–7096.
Lucadamo, L., Corapi, A., Loppi, S., De Rosa, R., Barca, D., Vespasiano, G., Gallo, L., 2015. Spatial variation in the accumulation of elements in thalli of the lichen *Pseudevernia furfuracea* (L.) Zopf transplanted around a biomass power plant in Italy. Arch. Environ. Contam. Toxicol.:1–16 http://dx.doi.org/10.1007/s00244-015-0238-4.
Magiera, T., Jabłońska, M., Strzyszcz, Z., Rachwal, M., 2011. Morphological and mineralogical forms of technogenic magnetic particles in industrial dusts. Atmos. Environ. 45, 4281–4290.
Magiera, T., Gołuchowska, B., Jabłońska, M., 2013. Technogenic magnetic particles in alkaline dusts from power and cement plants. Water Air Soil Pollut. 224:1389. http://dx.doi.org/10.1007/s11270-012-1389-9.
Marié, D.C., Chaparro, M.A.E., Irurzun, M.A., Lavornia, J.M., Marinelli, C., Cepeda, R., Böhnel, H.N., Castañeda Miranda, A.G., Sinito, A.M., 2016. Magnetic mapping of air pollution in Tandil city (Argentina) using the lichen *Parmotrema pilosum* as biomonitor. Atmos. Pollut. Res. 7, 513–520.
Moreno, E., Sagnotti, L., Dinarès-Turell, J., Winkler, A., Cascella, A., 2003. Biomonitoring of traffic air pollution in Rome using magnetic properties of tree leaves. Atmos. Environ. 37, 2967–2977.
Morris, W.A., Versteeg, J.K., Bryant, D.W., Legzdins, A.E., McCarry, B.E., Marvin, C.H., 1995. Preliminary comparisons between mutagenicity and magnetic susceptibility of respirable airborne particulate. Atmos. Environ. 29, 3441–3450.
Nascimbene, J., Tretiach, M., Corana, F., Lo, Schiavo F., Kodnik, D., Dainese, M., Mannucci, B., 2014. Patterns of traffic polycyclic aromatic hydrocarbon pollution in mountain areas can be revealed by lichen biomonitoring: a case study in the dolomites (eastern Italian Alps). Sci. Total Environ. 475, 90–96.
Paoli, L., Winkler, A., Guttová, A., Sagnotti, A., Grassi, A., Lackovičová, A., Senko, D., Loppi, S., 2016. Magnetic properties and element concentrations in lichens exposed to airborne pollutants released during cement production. Environ. Sci. Pollut. Res. http://dx.doi.org/10.1007/s11356-016-6203-6T.
Petrovský, E., Ellwood, B., 1999. Magnetic monitoring of air, land and water pollution. In: Maher, B.A., Thompson, R. (Eds.), Quaternary Climates, Environment and Magnetism. Cambridge University Press, pp. 279–322.
Pike, C.R., Roberts, A.P., Verosub, K.L., 1999. Characterizing interactions in fine magnetic particle systems using first order reversal curves. J. Appl. Phys. 85, 6660–6667.
Purvis, O.W., Chimonides, P.J., Jones, G.C., Mikhailova, I.N., Spiro, B., Weiss, D.J., Williamson, B.J., 2004. Lichen biomonitoring near Karabash smelter town, Ural mountains, Russia, one of the most polluted areas in the world. Proc. R. Soc. B 271, 221–226.
Quevauviller, P., Herzig, R., Muntau, H., 1996. Certified reference material of lichen (CRM 482) for the quality control of trace element bio-monitoring. Sci. Total Environ. 187, 143–152.
Revuelta, M.A., McIntosh, G., Pey, J., Pérez, N., Querol, X., Alastuey, A., 2014. Partitioning of magnetic particles in PM_{10}, $PM_{2.5}$ and PM_1 aerosols in the urban atmosphere of Barcelona (Spain). Environ. Pollut. 188, 109–117.
Roberts, A.P., Pike, C.R., Verosub, K.L., 2000. First-order reversal curve diagrams: a new tool for characterizing the magnetic properties of natural samples. J. Geophys. Res. 105, 28461–28475.
Sagnotti, L., Taddeucci, J., Winkler, A., Cavallo, A., 2009. Compositional, morphological, and hysteresis characterization of magnetic airborne particulate matter in Rome, Italy. Geochem. Geophys. Geosyst. 10. http://dx.doi.org/10.1029/2009GC002563.
Sagnotti, L., Winkler, A., 2012. On the magnetic characterization and quantification of the superparamagnetic fraction of traffic-related urban airborne PM in Rome, Italy. Atmos. Environ. 59, 131–140.
Salo, H., 2014. Preliminary enviromagnetic comparison of the moss, lichen, and filter fabric bags to air pollution monitoring. Fennia – Int. J. Geogr. 192, 154–163.
Salo, H., Bućko, M.S., Vaahtovuo, E., Limo, J., Mäkinen, J., Pesonen, L.J., 2012. Biomonitoring of air pollution in SW Finland by magnetic and chemical measurements of moss bags and lichens. J. Geochem. Explor. 115, 69–81.
Salo, H., Mäkinen, J., 2014. Magnetic biomonitoring by moss bags for industry-derived air pollution in SW Finland. Atmos. Environ. 97, 19–27.
Sorbo, S., Aprile, G., Strumia, S., Castaldo, Cobianchi R., Leone, A., Basile, A., 2008. Trace element accumulation in *Pseudevernia furfuracea* (L.) Zopf exposed in Italy's so called Triangle of Death. Sci. Total Environ. 407, 647–654.
Spiro, B., Weiss, D.J., Purvis, O.W., Mikhailova, I., Williamson, B.J., Coles, B.J., Udachin, V., 2004. Lead isotopes in lichen transplants around a Cu smelter in Russia determined by MC-ICP-MS reveal transient records of multiple sources. Environ. Sci. Technol. 38, 6522–6528.
Szönyi, M., Sagnotti, L., Hirt, A.M., 2007. On leaf magnetic homogeneity in particulate matter biomonitoring studies. Geophys. Res. Lett. 34. http://dx.doi.org/10.1029/2006GL029076.
Szönyi, M., Sagnotti, L., Hirt, A.M., 2008. A refined biomonitoring study of airborne particulate matter pollution in Rome, with magnetic measurements on *Quercus ilex* tree leaves. Geophys. J. Int. 173, 127–141.
Tretiach, M., Baruffo, L., 2001. Deposizione di metalli nella pedemontana pordenonese. Uno studio basato sui licheni come bioaccumulatori (Pordenone: Provincia di Pordenone).
Tretiach, M., Pittao, E., 2008. Biomonitoraggio di metalli mediante licheni in cinque aree campione della provincia di Pordenone. Stato attuale e confronto con i dati del 1999 (Pordenone: Provincia di Pordenone).
Tretiach, M., Crisafulli, P., Pittao, E., Rinino, S., Roccotiello, E., Modenesi, P., 2005. Isidia ontogeny and its effects on the CO_2 gas exchanges of the epiphytic lichen *Pseudevernia furfuracea* (L.) Zopf. Lichenologist 37, 445–462.
Tretiach, M., Adamo, P., Bargagli, R., Baruffo, L., Carletti, L., Crisafulli, P., Giordano, S., Modenesi, P., Orlando, S., Pittao, E., 2007. Lichen and moss bags as monitoring devices in urban areas. Part I: influence of exposure on sample vitality. Environ. Pollut. 146, 380–391.
Tretiach, M., Candotto, Carniel F., Loppi, S., Carniel, A., Bortolussi, A., Mazzilis, D., Del Bianco, C., 2011. Lichen transplants as a suitable tool to identify mercury pollution from waste incinerators: a case study from NE Italy. Environ. Monit. Assess. 175, 589–600.
Vuković, G., Aničić, Urošević M., Tomašević, M., Samson, R., Popović, A., 2015. Biomagnetic monitoring of urban air pollution using moss bags (*Sphagnum girgensohnii*). Ecol. Indic. 52, 40–47.
Wadleigh, M.A., 2003. Lichens and atmospheric sulphur: what stable isotopes reveal. Environ. Pollut. 126, 345–351.
Wang, X., Løvlie, R., Zhao, X., Yang, Z., Jiang, F., Wang, S., 2010. Quantifying ultrafine pedogenic magnetic particles in Chinese loess by monitoring viscous decay of superparamagnetism. Geochem. Geophys. Geosyst. 11. http://dx.doi.org/10.1029/2010GC003194.
Wiseman, R.D., Wadleigh, M.A., 2002. Lichen response to changes in atmospheric sulphur: isotopic evidence. Environ. Pollut. 116, 235–241.
WHO (World Health Organization), 2005. Air quality guidelines for particulate matter, ozone, nitrogen dioxide and sulfur dioxide. Global Update 2005, Summary of Risk Assessment. WHO Press, Geneva, Switzerland.
WHO (World Health Organization), 2014. Fact sheet no. 313: ambient (outdoor) air quality and health. http://www.who.int/mediacentre/factsheets/fs313/en/.
WHO (World Health Organization), 2016. http://www.who.int/gho/phe/outdoor_air_pollution/en/, last visit 8th February 2016.
Zhang, C., Huang, B., Li, Z., Liu, H., 2006. Magnetic properties of high-road-side pine tree leaves in Beijing and their environmental significance. Chin. Sci. Bull. 51, 3041–3052.
Zhang, C., Huang, B., Piper, J.D.A., Luo, R., 2008. Biomonitoring of atmospheric particulate matter using magnetic properties of *Salix matsudana* tree ring cores. Sci. Total Environ. 393, 177–190.